

Galactic Globular Clusters as a test for Very Low-Mass stellar models.

S. Cassisi^{1,2}, V. Castellani^{1,3}, P. Ciarcelluti^{1,4}, G. Piotto⁵ and M. Zoccali⁵

¹ *Osservatorio Astronomico di Collurania, Via M. Maggini, I-64100, Teramo, Italy - E-Mail: cassisi@astr.te.astro.it*

² *Max-Planck-Institut für Astrophysik, Karl-Schwarzschild-Strasse 1, D-85740 Garching, Germany*

³ *Università degli Studi di Pisa, Dipartimento di Fisica, Piazza Torricelli, I-56100, Pisa, Italy; vittorio@astr18pi.difi.unipi.it*

⁴ *Università degli studi de L'Aquila, Dipartimento di Fisica, Via Vetoto, I-67100, L'Aquila, Italy*

⁵ *Università di Padova, Dipartimento di Astronomia, Vicolo dell'Osservatorio 5, 35122 Padova, Italy;*

piotto@pd.astro.it; manu@obelix.pd.astro.it

ABSTRACT

We make use of the Next Generation model atmospheres by Allard et al. (1997) and Hauschildt, Allard & Baron (1999) to compute theoretical models for low and very low-mass stars for selected metallicities in the range $Z = 0.0002$ to 0.002 . On this basis, we present theoretical predictions covering the sequence of H-burning stars as observed in galactic globulars from the faint end of the Main Sequence up to, and beyond, the cluster Turn Off. The role played by the new model atmospheres is discussed, showing that present models appear in excellent agreement with models by Baraffe et al. (1997) as computed on quite similar physical basis. One finds that the theoretical mass - luminosity relations based on this updated set of models, are in good agreement with the empirical data provided by Henry & McCarthy (1993). Comparison with HST observation discloses that the location in the Color-Magnitude diagram of the lower Main Sequence in galactic globular clusters appears again in good agreement with the predicted sensitive dependence of these sequences on the cluster metallicity.

Key words: stars: evolution – stars: interiors – globular clusters: general

1 INTRODUCTION

Very Low Mass (VLM) stars play a relevant role in a wide variety of astrophysical problems, ranging from the stellar formation processes to the stellar interior physics and from the Galaxy formation to the cosmological Dark Matter enigma. Therefore, in the last decade large efforts have been devoted to increase the wealth of low-mass and VLM stars observations both in the visual and near-infrared bands. A substantial progress in this field has been recently achieved thanks to the HST observations which disclosed in several galactic globular clusters (GCs) a beautiful sequence of central H-burning stars (Piotto et al. 1997, Ferraro et al. 1997, Marconi et al. 1998), sometimes nearly down to the lower mass limit for hydrogen burning structures (King et al. 1998).

The theoretical modeling of VLM stars has been for a long time quite a difficult task, due to the high densities and the low temperatures which characterize the structure of these stars. As a consequence, reliable theoretical predictions on both effective temperature and luminosity, as needed to understand the Color-Magnitude (CM) diagram of VLM stars, have been for long time severely challenged. However, in the last years the situation has significantly improved thanks to the relevant progress both in the physics

of the stellar interiors as well as in the treatment of the stellar atmospheric layers (for a detailed review on this topic see Allard et al. 1997). As a result, theoretical investigations based on this new physical framework have been already able to achieve a satisfactory agreement with several observational evidences (see Kroupa & Tout 1997, Baraffe et al. 1997, hereinafter BCHA97, Chabrier & Baraffe 1997, Brocato, Cassisi & Castellani 1998, hereinafter BCC98, and references therein).

This is the third of a series of papers (see Alexander et al. 1997 and BCC98) devoted to investigate VLM structures: in the first paper (Alexander et al. 1998), we have investigated the effect of using the most updated physical inputs - as far as it concerns the equation of state and the low-temperature opacity - on the theoretical prescriptions for VLM stars; the second one (BCC98) analyzed the effects on the evolutionary models of the different approaches adopted for fixing the outer boundary conditions in stellar structure computations.

In the present work, we will take advantage of the recent availability of the "Next Generation" (NG) model atmospheres provided by Allard et al. (1997) and Hauschildt et al. (1999) to discuss the effects of such new improved boundary conditions on stellar models for VLM structures.

We will show that the structure of theoretical models appears scarcely affected by the choice about these conditions. However, this is not the case for the predicted colours, which strongly depend on the adopted relation connecting the theoretical quantities, as luminosity (L) and effective temperature (T_e) to the observational ones as magnitudes and colours. Not surprisingly, present models, as computed on the basis of the NG model atmospheres, appear to be in excellent agreement with the result of similar computations given by BCAH97.

We will also take advantage of the growing number of detailed VLM sequences in galactic GCs provided by HST to extend the comparison from NGC6397 to other, now well observed, GCs disclosing that observational data are largely supporting theoretical predictions concerning the dependence on the metallicity of the CM diagram location of VLM sequences. The layout of this paper is as follows: as a preliminary step, in the next section we present updated VLM models, discussing to some extent these results to the light of the current uncertainties on the mixing length parameter and/or the cluster age. On this basis, section 3 will be devoted to a comparison with observations, pointing out the use of the VLM Main Sequence (MS) as possible calibrator of the cluster metallicity and/or distance modulus. Conclusions and final remarks will close the paper.

2 THE STELLAR MODELS

As in the previous papers (Alexander et al. 1997, and BCC98) our models rely on the equation of state by Saumon et al. (1995) for dense and cool matter, on low-temperature opacities by Alexander & Ferguson (1994) and high-temperature opacities by Rogers & Iglesias (1992). As already quoted, in BCC98 the outer boundary conditions were fixed by adopting model atmospheres by Brett (1995a,b). In this paper we will follow BCAH97 in using NG model atmospheres, which represent a significant improvement in this field, due to the use of an updated treatment of pressure broadening and of molecular line absorption coefficients (see Allard et al. 1997, and Hauschildt et al. 1999 for more details). As in BCC98, the basis of the atmosphere has been fixed at Rosseland optical depth $\tau = 100$, i.e., at a depth large enough for the diffusion approximation to be valid (see, e.g., Mihalas 1978, Morel et al. 1994), allowing a safe comparison with the results of different authors.

VLM models have been computed for selected metallicity values, as given by $Z=0.0002$, 0.0006 , 0.001 and 0.002 , by adopting in all cases an original helium abundance $Y = 0.23$. In order to cover with a homogeneous and self-consistent theoretical scenario the upper portion of the MS and the cluster Turn Off (TO), numerical computations have been extended beyond the proper VLM range, up to $M \sim 0.8M_\odot$, adopting for masses larger than $0.6M_\odot$ the OPAL EOS (Rogers, Swenson & Iglesias 1996) which allow the required fine match with the VLM sequence (see Brocato, Cassisi & Castellani 1997 for a discussion on this matter). Tables 1 to 4 provide relevant informations about the models, as computed assuming a mixing length parameter $ml = 1.8H_P$ and a cluster age of 10 Gyr. According to the solar bolometric correction adopted by Allard et al. (1997), we used $M_{Bol,\odot} = 4.73$ mag to derive VRI magnitudes in the Johnson-Cousins system and JHK ones in the CIT system. In addition, we

provide the stellar magnitudes in some selected HST filters, including the NICMOS wide filters F110W, F160W and F807W.

Figure 1 shows the location in the theoretical HR diagram of the new models with $Z=0.0002$ and 0.002 , as compared with similar models provided by BCC98, BCAH97 as well as with models computed by adopting a $T(\tau)$ relation in the atmospheric layers. As whole, models in this figure appear all in reasonable agreement; this occurrence shows that the thermal structures of the models is not dramatically dependent on the adopted boundaries conditions. As expected, one finds that the new models based on NG model atmospheres are virtually identical with those by BCAH97, showing that different groups with different evolutionary codes obtain results which only depend on the adopted input physics. One may finally notice that Brett's (1995a,b) model atmospheres provided a description of the thermal structure of VLM stars which is comparable with the most updated NG models over a rather large range of effective temperatures. However, in the region around $\log T_e \sim 3.63$ the new models based on the NG model atmospheres appear slightly hotter and marginally more luminous than the ones computed by adopting the boundary conditions given by Brett (1995a,b). As discussed by Bessel (1995), such a difference is probably due to the too strong H_2O bands in Brett's model atmospheres, which produces an overestimate of the H_2O opacity for temperatures cooler than 3000K.

However, it is worth noticing that the colour - effective temperature relations based on different model atmospheres databases, show remarkable differences. This is shown in figure 2 where we compare VLM sequences in the observational ($M_V, V - I$) diagram for selected metallicities, as evaluated by adopting alternatively the bolometric corrections and colour - effective temperature relations provided either by the NG model atmospheres or by Allard & Hauschildt's (1995) (implemented at effective temperatures larger than 4000K with the Kurucz's (1993) transformations), as in BCC98. The significant differences between the two approaches show that whereas model atmospheres are already good enough to produce reliable stellar models, the prediction about colours is still uncertain, affected by even minor details in the evaluation of predicted spectra. In this field, the NG model atmospheres represent a significant improvement in comparison with the previous theoretical results.

Present theoretical predictions concerning the CMD location of VLM sequences are reported in figure 3 for the four selected metallicities and for an assumed cluster age of 10 Gyr. As already known, one finds that at lower luminosities the VLM sequence is predicted to be a rather sensitive indicator of the cluster metallicity. As a relevant point, numerical experiments fully support the BCAH97's finding that the VLM sequence for magnitudes below $M_V \sim 7$ mag is expected to be strictly independent of assumptions about either the cluster age or the efficiency of super-adiabatic convection. One concludes that the run of VLM sequences in the CM diagram is among the "not-too-abundant" observational quantities firmly predicted by theory, only depending on the reliability of the adopted physical scenario.

Figure 4 finally gives the mass - luminosity relations for all the investigated metallicities and for selected photometric bands ranging from the visual to the near-infrared. It is

Figure 1. The H-R diagram location of present VLM models with mass $\leq 0.6M_{\odot}$ and for an age of 10Gyr, as compared with the models by Baraffe et al. (1997) or Brocato et al. (1998) for the labeled assumptions on the metallicity. Dotted lines shows models computed by adopting the same input physics used in this work but a gray approximation ($T(\tau)$ relation) in the treatment of the outer layers.

Figure 2. The predicted location in the $(M_V, V - I)$ CM diagram of VLM sequence from the present paper (points) and from BCAH97 (solid line) according to evaluations of colours based on the NG model atmospheres, and for two assumptions about the stellar metallicity: $Z=0.0002$ and 0.002 . Dotted lines show the location of the same theoretical sequences but adopting Allard and Hauschildt's (1995) colours (see text).

worth noticing (see also BCC98) that the mass - luminosity relation becomes more and more insensitive to the stellar metallicity when going from the visual to the near-infrared

Figure 3. Comparison between theoretical isochrones in the $(M_V, V - I)$ diagram for an age 10Gyr and for the labeled assumptions about the metallicity.

photometric bands, with the $m - M_K$ relation almost unaffected by the metallicity. This occurrence together with the evidence that in the near-IR the effects of extinction and differential reddening are considerably reduced, can be of help when investigating the mass distribution of VLM objects in the field and in the galactic bulge (see for instance, Zoccali et al. 1999). In the same figure, the empirical data by Henry

Table 1. Mass, luminosity, effective temperature, absolute visual magnitude, colours and magnitudes in selected HST filters for stellar models with metallicity $Z=0.0002$ and $Y=0.23$ and for an age 10 Gyr.

M/M_{\odot}	$\log L/L_{\odot}$	$\log T_e$	M_V	$(V-I)$	$(V-R)$	$(V-K)$	$(I-J)$	$(J-H)$	M_{555}	M_{606}	M_{814}	M_{110W}	M_{160W}	M_{807W}
.095	-3.182	3.473	14.771	2.801	1.331	4.063	1.200	.154	14.725	14.095	11.960	11.077	10.536	10.681
.096	-3.137	3.481	14.558	2.688	1.277	4.012	1.193	.194	14.508	13.900	11.857	10.989	10.412	10.526
.097	-3.095	3.488	14.373	2.596	1.236	3.978	1.186	.229	14.322	13.729	11.760	10.907	10.299	10.384
.098	-3.057	3.495	14.198	2.507	1.197	3.939	1.177	.261	14.148	13.569	11.673	10.833	10.199	10.257
.099	-3.021	3.501	14.040	2.429	1.163	3.899	1.170	.288	13.988	13.423	11.589	10.761	10.104	10.143
.100	-2.989	3.506	13.902	2.365	1.137	3.863	1.163	.310	13.850	13.296	11.515	10.696	10.021	10.045
.101	-2.959	3.511	13.772	2.303	1.111	3.827	1.156	.330	13.719	13.173	11.446	10.636	9.945	9.953
.102	-2.931	3.515	13.658	2.253	1.092	3.798	1.149	.347	13.604	13.065	11.380	10.578	9.874	9.871
.104	-2.882	3.522	13.461	2.170	1.061	3.746	1.137	.373	13.406	12.876	11.265	10.476	9.753	9.730
.107	-2.819	3.530	13.223	2.081	1.031	3.685	1.122	.399	13.167	12.644	11.114	10.341	9.599	9.557
.110	-2.765	3.537	13.022	2.009	1.009	3.630	1.107	.419	12.964	12.446	10.984	10.224	9.470	9.413
.112	-2.734	3.541	12.909	1.970	.998	3.599	1.098	.429	12.850	12.334	10.909	10.156	9.397	9.332
.115	-2.690	3.546	12.757	1.924	.986	3.562	1.087	.440	12.697	12.182	10.801	10.059	9.293	9.219
.120	-2.623	3.553	12.533	1.864	.971	3.509	1.071	.453	12.474	11.957	10.637	9.909	9.137	9.049
.125	-2.566	3.559	12.344	1.815	.958	3.462	1.055	.462	12.285	11.768	10.495	9.781	9.005	8.907
.130	-2.515	3.564	12.177	1.775	.947	3.420	1.041	.469	12.119	11.602	10.368	9.664	8.888	8.783
.140	-2.426	3.572	11.894	1.715	.927	3.353	1.018	.477	11.836	11.324	10.144	9.459	8.683	8.566
.150	-2.347	3.578	11.651	1.670	.908	3.303	1.001	.482	11.595	11.089	9.946	9.275	8.501	8.374
.160	-2.277	3.584	11.432	1.627	.887	3.250	.983	.485	11.377	10.880	9.768	9.112	8.342	8.207
.180	-2.153	3.592	11.063	1.571	.857	3.179	.958	.487	11.010	10.527	9.454	8.816	8.053	7.910
.200	-2.045	3.598	10.749	1.530	.833	3.123	.939	.488	10.697	10.226	9.181	8.556	7.798	7.651
.220	-1.953	3.603	10.481	1.495	.813	3.074	.922	.488	10.432	9.971	8.947	8.335	7.582	7.433
.250	-1.836	3.609	10.144	1.454	.788	3.011	.903	.487	10.096	9.650	8.651	8.054	7.308	7.156
.300	-1.682	3.617	9.701	1.400	.755	2.925	.876	.483	9.656	9.226	8.261	7.683	6.948	6.796
.350	-1.560	3.623	9.355	1.361	.731	2.858	.856	.480	9.310	8.893	7.952	7.389	6.662	6.512
.400	-1.444	3.629	9.022	1.322	.708	2.790	.837	.476	8.980	8.575	7.658	7.110	6.392	6.245
.450	-1.298	3.640	8.585	1.253	.667	2.667	.802	.468	8.544	8.162	7.288	6.765	6.065	5.924
.500	-1.123	3.656	8.051	1.159	.611	2.491	.753	.452	8.012	7.661	6.848	6.361	5.686	5.557
.600	-.693	3.719	6.737	.868	.447	1.871	.568	.363	6.696	6.438	5.818	5.458	4.918	4.837
.650	-.486	3.751	6.172	.750	.383	1.604	.487	.320	6.128	5.906	5.368	5.064	4.587	4.528
.700	-.277	3.778	5.630	.657	.334	1.393	.423	.284	5.583	5.389	4.916	4.655	4.231	4.188
.800	.227	3.826	4.340	.489	.248	1.010	.311	.200	4.288	4.144	3.788	3.600	3.291	3.273

Table 2. As Table 1 but for stellar models with metallicity $Z=0.0006$.

M/M_{\odot}	$\log L/L_{\odot}$	$\log T_e$	M_V	$(V-I)$	$(V-R)$	$(V-K)$	$(I-J)$	$(J-H)$	M_{555}	M_{606}	M_{814}	M_{110W}	M_{160W}	M_{807W}
.0929	-3.292	3.444	15.985	3.550	1.688	5.234	1.479	.267	15.956	15.264	12.471	11.346	10.667	10.806
.0930	-3.288	3.445	15.955	3.530	1.676	5.217	1.476	.271	15.925	15.236	12.459	11.338	10.656	10.791
.0940	-3.242	3.453	15.673	3.367	1.581	5.086	1.449	.308	15.644	14.983	12.334	11.245	10.533	10.641
.0950	-3.199	3.461	15.404	3.209	1.494	4.957	1.421	.341	15.374	14.737	12.216	11.160	10.420	10.501
.1000	-3.028	3.490	14.434	2.680	1.236	4.510	1.317	.446	14.393	13.830	11.755	10.812	9.995	9.988
.1100	-2.820	3.518	13.489	2.264	1.073	4.125	1.221	.511	13.441	12.920	11.208	10.361	9.505	9.432
.1200	-2.686	3.533	12.965	2.084	1.016	3.937	1.169	.531	12.914	12.404	10.859	10.058	9.198	9.097
.1300	-2.581	3.543	12.592	1.980	.987	3.816	1.135	.537	12.540	12.031	10.587	9.814	8.959	8.841
.1500	-2.409	3.559	12.004	1.833	.952	3.631	1.080	.535	11.949	11.439	10.141	9.413	8.575	8.434
.1700	-2.275	3.570	11.571	1.744	.928	3.505	1.042	.530	11.516	11.007	9.794	9.096	8.273	8.121
.2000	-2.107	3.581	11.057	1.660	.898	3.380	1.003	.523	11.004	10.504	9.363	8.694	7.889	7.726
.2500	-1.897	3.592	10.441	1.579	.861	3.250	.964	.516	10.389	9.905	8.825	8.186	7.398	7.231
.3000	-1.741	3.599	9.996	1.531	.835	3.169	.940	.514	9.944	9.473	8.428	7.806	7.027	6.860
.3500	-1.618	3.605	9.642	1.489	.812	3.099	.919	.512	9.591	9.133	8.114	7.507	6.735	6.569
.4000	-1.495	3.612	9.282	1.441	.785	3.017	.896	.510	9.232	8.789	7.801	7.212	6.447	6.283
.4500	-1.341	3.623	8.819	1.368	.742	2.895	.864	.511	8.771	8.351	7.411	6.846	6.088	5.931
.5000	-1.158	3.640	8.248	1.255	.678	2.711	.817	.512	8.200	7.817	6.949	6.421	5.671	5.528
.5500	-.956	3.668	7.573	1.084	.580	2.401	.738	.482	7.524	7.198	6.442	5.973	5.269	5.148
.5800	-.836	3.688	7.175	.982	.518	2.175	.671	.440	7.129	6.834	6.143	5.719	5.073	4.970
.6000	-.724	3.708	6.823	.896	.467	1.965	.604	.397	6.779	6.512	5.876	5.496	4.912	4.826
.6500	-.518	3.742	6.236	.773	.399	1.661	.505	.335	6.192	5.962	5.410	5.095	4.597	4.536
.7000	-.314	3.769	5.703	.682	.349	1.447	.439	.295	5.655	5.454	4.964	4.694	4.254	4.209
.8000	.157	3.813	4.509	.533	.271	1.104	.337	.228	4.455	4.300	3.915	3.710	3.367	3.346

Table 3. As Table 1 but for stellar models with metallicity $Z=0.001$.

M/M_{\odot}	$\log L/L_{\odot}$	$\log T_e$	M_V	$(V-I)$	$(V-R)$	$(V-K)$	$(I-J)$	$(J-H)$	M_{555}	M_{606}	M_{814}	M_{110W}	M_{160W}	M_{807W}
.0917	-3.354	3.429	16.687	3.956	1.915	5.878	1.663	.306	16.659	15.935	12.781	11.501	10.775	10.921
.0920	-3.339	3.432	16.577	3.891	1.872	5.817	1.647	.318	16.550	15.838	12.735	11.470	10.734	10.871
.0930	-3.292	3.440	16.267	3.713	1.759	5.654	1.609	.352	16.241	15.561	12.598	11.373	10.609	10.721
.0940	-3.249	3.448	15.971	3.541	1.655	5.493	1.569	.383	15.946	15.293	12.471	11.284	10.498	10.585
.0950	-3.209	3.455	15.711	3.393	1.570	5.355	1.534	.409	15.685	15.054	12.353	11.201	10.396	10.461
.0960	-3.171	3.462	15.458	3.248	1.490	5.217	1.499	.432	15.431	14.820	12.241	11.124	10.301	10.345
.0980	-3.103	3.473	15.045	3.022	1.373	5.003	1.446	.467	15.012	14.432	12.045	10.982	10.135	10.147
.1000	-3.045	3.483	14.695	2.833	1.283	4.817	1.398	.493	14.659	14.100	11.876	10.861	9.997	9.983
.1050	-2.930	3.499	14.112	2.559	1.169	4.542	1.327	.527	14.073	13.540	11.555	10.611	9.728	9.675
.1100	-2.843	3.510	13.713	2.391	1.105	4.363	1.281	.544	13.670	13.151	11.317	10.416	9.528	9.452
.1200	-2.711	3.524	13.178	2.203	1.041	4.151	1.223	.557	13.132	12.625	10.961	10.114	9.225	9.125
.1300	-2.607	3.535	12.777	2.076	1.003	3.996	1.180	.560	12.728	12.225	10.683	9.873	8.992	8.874
.1500	-2.438	3.550	12.184	1.923	.965	3.794	1.122	.555	12.132	11.628	10.236	9.474	8.611	8.472
.2000	-2.134	3.573	11.203	1.727	.917	3.503	1.036	.537	11.149	10.644	9.444	8.751	7.926	7.762
.2500	-1.921	3.585	10.568	1.637	.885	3.358	.992	.527	10.515	10.021	8.897	8.236	7.431	7.260
.3000	-1.764	3.593	10.111	1.579	.859	3.261	.964	.521	10.058	9.576	8.495	7.855	7.063	6.890
.3500	-1.640	3.598	9.759	1.542	.841	3.197	.946	.519	9.707	9.234	8.180	7.553	6.768	6.594
.4000	-1.516	3.605	9.394	1.493	.815	3.112	.921	.516	9.343	8.883	7.862	7.254	6.478	6.306
.4500	-1.361	3.616	8.929	1.422	.777	2.993	.888	.518	8.878	8.440	7.467	6.884	6.113	5.948
.5000	-1.181	3.632	8.373	1.317	.718	2.827	.847	.529	8.321	7.918	7.013	6.464	5.691	5.538
.5500	-.979	3.659	7.693	1.140	.618	2.530	.776	.517	7.639	7.295	6.508	6.014	5.264	5.137
.6000	-.752	3.698	6.923	.936	.494	2.076	.642	.429	6.876	6.596	5.936	5.534	4.906	4.811
.6500	-.549	3.733	6.318	.801	.417	1.736	.530	.353	6.272	6.033	5.463	5.132	4.610	4.540
.7000	-.349	3.761	5.786	.704	.364	1.502	.456	.310	5.739	5.530	5.026	4.744	4.286	4.239
.8000	.099	3.804	4.640	.560	.288	1.167	.357	.237	4.588	4.423	4.020	3.804	3.444	3.417

Table 4. As Table 1 but for stellar models with metallicity $Z=0.002$.

M/M_{\odot}	$\log L/L_{\odot}$	$\log T_e$	M_V	$(V-I)$	$(V-R)$	$(V-K)$	$(I-J)$	$(J-H)$	M_{555}	M_{606}	M_{814}	M_{110W}	M_{160W}	M_{807W}
.0894	-3.473	3.401	17.982	4.596	2.287	7.028	2.094	.363	17.952	17.149	13.436	11.809	11.008	11.198
.0895	-3.468	3.402	17.943	4.576	2.274	7.004	2.086	.366	17.914	17.115	13.418	11.798	10.995	11.182
.0897	-3.457	3.404	17.864	4.535	2.246	6.957	2.069	.373	17.835	17.047	13.379	11.773	10.965	11.148
.0900	-3.441	3.407	17.746	4.473	2.204	6.886	2.045	.384	17.718	16.945	13.323	11.738	10.923	11.098
.0910	-3.392	3.416	17.388	4.285	2.077	6.672	1.974	.414	17.363	16.633	13.152	11.630	10.794	10.946
.0920	-3.346	3.425	17.037	4.094	1.951	6.458	1.904	.442	17.014	16.323	12.992	11.530	10.675	10.802
.0930	-3.304	3.432	16.746	3.940	1.851	6.290	1.851	.463	16.724	16.062	12.853	11.437	10.568	10.675
.0950	-3.227	3.446	16.186	3.634	1.663	5.954	1.747	.500	16.165	15.551	12.595	11.271	10.377	10.443
.0970	-3.159	3.458	15.712	3.380	1.516	5.670	1.661	.526	15.690	15.112	12.371	11.123	10.214	10.246
.1000	-3.074	3.471	15.176	3.106	1.371	5.362	1.572	.551	15.151	14.607	12.103	10.935	10.014	10.012
.1100	-2.882	3.497	14.127	2.623	1.161	4.789	1.406	.581	14.094	13.586	11.520	10.503	9.575	9.512
.1200	-2.752	3.511	13.545	2.403	1.081	4.515	1.328	.587	13.507	13.010	11.147	10.201	9.280	9.189
.1300	-2.649	3.521	13.125	2.265	1.037	4.333	1.276	.586	13.084	12.593	10.859	9.960	9.047	8.939
.1500	-2.483	3.536	12.499	2.087	.987	4.085	1.204	.580	12.454	11.966	10.402	9.566	8.672	8.542
.1700	-2.349	3.547	12.029	1.973	.960	3.915	1.154	.570	11.981	11.491	10.040	9.247	8.371	8.227
.2000	-2.177	3.560	11.454	1.849	.935	3.721	1.097	.555	11.403	10.907	9.582	8.836	7.986	7.825
.2500	-1.964	3.573	10.794	1.739	.911	3.541	1.044	.542	10.742	10.245	9.026	8.324	7.495	7.322
.3000	-1.804	3.581	10.321	1.675	.894	3.435	1.012	.535	10.269	9.775	8.613	7.937	7.121	6.943
.3500	-1.678	3.587	9.955	1.631	.878	3.357	.989	.532	9.902	9.413	8.290	7.632	6.824	6.644
.4000	-1.552	3.593	9.591	1.588	.860	3.283	.967	.530	9.538	9.057	7.968	7.326	6.525	6.344
.4500	-1.402	3.602	9.148	1.527	.833	3.180	.938	.531	9.096	8.628	7.584	6.965	6.167	5.990
.5000	-1.223	3.619	8.583	1.415	.777	3.004	.891	.549	8.529	8.093	7.128	6.547	5.745	5.578
.5500	-1.031	3.642	7.954	1.262	.698	2.771	.839	.564	7.893	7.508	6.647	6.110	5.301	5.154
.6000	-.834	3.674	7.250	1.057	.577	2.377	.737	.509	7.193	6.874	6.144	5.682	4.947	4.831
.6500	-.611	3.715	6.508	.867	.458	1.910	.590	.399	6.460	6.199	5.588	5.221	4.635	4.553
.7000	-.417	3.744	5.955	.760	.398	1.638	.501	.338	5.907	5.680	5.141	4.831	4.330	4.269
.8000	-.005	3.787	4.884	.613	.318	1.287	.392	.262	4.833	4.652	4.213	3.974	3.579	3.545

& McCarthy (1993) for a sample of visual and eclipsing binaries in the solar neighborhood are also shown. Since such a sample is expected to cover a significant spread in metallicity, fig. 4 has been implemented with the theoretical mass - luminosity relation for solar composition, as computed by

using the same physical inputs adopted for the more metal poor VLM sequences. One can easily notice that, within the current uncertainties and the significant dispersion (due to a spread in the metallicity and, probably also in the age) in the observational data, there is a quite good agreement be-

Figure 4. The mass - luminosity relations for various assumptions on the heavy elements abundance, in selected photometric bands. The observational data provided by Henry & McCarthy (1993) are also shown. The mass - luminosity relation corresponding to solar metallicity VLM models has been also plotted (see text for more details).

tween empirical and theoretical mass - luminosity relations.

3 THE OBSERVATIONAL TEST

BCAH97 were already able to test their prediction to the high quality CM diagram of NGC6397 (Cool, Piotto & King 1996). Unfortunately, a similar precise comparisons with clusters of different metallicities (M15 and ω Cen) was hampered by the poorer quality of photometric data available at that time. However, the sample of VLM sequences observed by HST in galactic globulars is increased, and now one finds five more clusters with sufficiently well defined VLM sequences, as given by M92, M30 (Piotto et al. 1997), NGC6752 (Ferraro et al. 1997), M10 and M55 (Piotto & Zoccali 1999). Table 5 gives estimates of $[\text{Fe}/\text{H}]$ for this sample of "well observed" clusters as provided by Cohen et al. (1999). The same table gives the values of the global metallicity $[\text{M}/\text{H}]$ as obtained by adopting the prescription for the relation between $[\text{Fe}/\text{H}]$, $[\alpha/\text{Fe}]$, and $[\text{M}/\text{H}]$ provided by Salaris, Chieffi & Straniero (1993) and assuming alternatively $[\alpha/\text{Fe}]=-0.25$ ($[\text{M}/\text{H}]_{0.25}$) and $[\alpha/\text{Fe}]=-0.35$ ($[\text{M}/\text{H}]_{0.35}$), in order to take into account the current uncertainty in the α -elements enhancement in GC stars. Current estimates for

Figure 5. The CMDs of NGC6752 and M30 with the CMD of NGC6752 shifted to overlap the Turn Off of M30 (see text).

Figure 6. Comparison between the HST CMD of NGC6397 and the theoretical isochrones. The solid lines correspond to the evolutionary prescriptions for the metallicity adopted for the cluster, and the dashed lines show the main sequence loci for very low-mass structures, for all the other metallicities accounted for in the present work. The age of the various isochrones, the adopted distance modulus and reddening are also labeled.

distance modulus and reddening taken from the compilation of Harris (1996) are also listed.

However, as shown in the same table, three clusters out of this sample (M92, M55 and M10) have been observed with the HST F606W filter, so that data are not homogeneous with NGC6397 and, in addition, their calibration can be affected by not negligible uncertainties. Thus we will limit the following discussion only to the three clusters M30, NGC6397 and NGC6752. The observational data for these

Table 5. Heavy element abundance and selected observational parameters for globular clusters with "well observed" VLM sequence.

NGC	Name	HST filters	[Fe/H] _C	[M/H] _{0.25}	[M/H] _{0.35}	E(V - I)	(m - M) _V
6341	M92	F606W, F814W	-2.10	-1.93	-1.85	0.03	14.64
7099	M30	F555W, F814W	-1.94	-1.77	-1.69	0.04	14.62
6397		F555W, F814W	-1.78	-1.61	-1.53	0.24	12.36
6809	M55	F606W, F814W	-1.65	-1.47	-1.40	0.09	13.87
6752		F555W, F814W	-1.41	-1.24	-1.16	0.05	13.13
6254	M10	F606W, F814W	-1.38	-1.21	-1.13	0.38	14.08

Figure 7. As figure 6 but for the cluster M30.

clusters have been translated from the HST photometric system to the standard Johnson-Cousins system by adopting the Holtzman et al. (1995) recipes.

As a first crude test of the metal dependence predicted by theory, let us show in figure 5 the data for NGC6752, the more metal-rich cluster in our sample, shifted onto the M30 data in such a way that the location of the Turn Off points in both clusters coincides. Comparison with theoretical predictions given in figure 3, shows that there is a clear evidence for the existence of the effect of metallicity on the location of the lower main sequences - with a shift toward redder colours when increasing the metallicity -, which appears in good, even if qualitative, agreement with theoretical predictions.

A precise comparison between observations and theoretical predictions would require an exact knowledge of both the cluster reddening and distance modulus. As a less stringent but still significant approach, one can adopt, e.g., a suitable value for the cluster reddening, regarding the distance modulus as a free parameter to be determined by best fitting theoretical predictions: the accuracy of the fitting all along the MS will be a non trivial indicator of the reliability of the theoretical scenario. As a first application of this last procedure, let us follow BCAH97 assuming for NGC6397, $E(B - V) = 0.18$ which corresponds to $E(V - I) = 0.24$ by adopting the relation $E(V - I) = 1.35 \cdot E(B - V)$ (Drukier

et al. 1993, He et al. 1995). Not surprisingly, figure 6 shows that a good fit is achieved adopting $[M/H] = -1.5$ and $(m - M)_0 = 11.9$ (corresponding to $(m - M)_V = 12.46$), as already found by BCAH97. The run of VLM sequences for different metallicities, as given in the same figure, discloses the good sensitivity of this fitting to the assumed metal content. One may notice that the derived distance modulus is in satisfactory agreement with the independent evaluation given by Reid & Gizis (1998) on the basis of Hipparcos M-subdwarf Main-Sequence fitting.

In addition, now one can note that the comparison of the cluster Turn-Off luminosity with theoretical isochrones as computed for selected ages and without allowing for the efficiency of element sedimentation (see Cassisi et al. 1998, 1999) would assign to the cluster an age of, about, 12 Gyr, in good agreement with the age recently discussed on quite an independent way by Salaris & Weiss (1997). If element diffusion is at work in Pop. II globular cluster stars, thus the age of the cluster would be further reduced by an additional ~ 0.7 Gyr (see Castellani et al. 1997, Cassisi et al. 1998, 1999). However, one has also to bear in mind that the derived age is dependent on the assumption about the cluster reddening: if the reddening is reduced by $\Delta E(V - I) \sim 0.03$ the age estimated for the cluster is increased by ~ 1 Gyr.

One can take advantage of the range of metallicities covered by our cluster sample to explore theoretical predictions in a rather large range of metallicities. Figure 7 shows that adopting for M30 $E(B - V) = 0.03$ and thus $E(V - I) = 0.04$ from the Harris's compilation, the fitting of the cluster loci by the theoretical sequence for $[M/H] = -2.0$ requires a distance modulus equal to $(m - M)_V = 14.98$, which is about 0.3 mag larger than the value listed in the Harris's compilation, but in good agreement with the value recently given by Gratton et al (1997: $(m - M)_V = 14.94 \pm 0.08$) obtained from the main-sequence fitting to Hipparcos subdwarfs. By comparing the theoretical prescriptions for the TO luminosity with the cluster CM diagram, one predicts for this cluster again an age of the order of 12 Gyr.

Figure 8 (top panel) shows the result of the same procedure but for the cluster NGC6752. Assuming again from Harris data $E(B - V) = 0.04$, i.e. $E(V - I) = 0.05$, and adopting a metallicity $[M/H] = -1.3$, the best fit is achieved for a distance modulus equal to $(m - M)_V = 13.08$, in reasonable agreement with the value given by Harris (1996) and with the estimate given by Renzini et al. (1996) from the white dwarfs cooling sequence, but smaller by about 0.1 mag than the determination by Gratton et al. (1997). From this figure, it is easy to notice that the observed lower main-sequence location seems to be in better agreement with the theoretical prescriptions for a metallicity $[M/H] \sim -1.0$

rather than with $[M/H]=-1.3$. This occurrence can be due to several reasons: problems in the calibration of the observational data from the HST photometry to the standard system and/or drawbacks in the adopted colour - effective temperature relation for this moderately metal-rich mixture, and/or the uncertainty in the estimation of the global metallicity suitable for the cluster (see table 5). It is also surprising to notice that the fitting given in Figure 8 (top panel) implies a cluster age larger or of the order of 14 Gyr, and one is reluctant to conclude for such large age. In order to reduce this age down to ~ 12 Gyr, the cluster reddening would have to be doubled and this choice is not supported by current determinations of such a parameter. However, the cluster age could be significantly reduced if, as suggested by the VLM sequence, we accept for the cluster a metallicity $[M/H] \sim -1.0$ - a value larger than the one usually adopted for this GC -, since increasing the metallicity decreases the magnitude of the Turn-Off for each given cluster age. This has been done in the bottom panel of figure 8, where we compare the CM diagram of NGC6752 with the theoretical isochrones corresponding to a stellar metallicity $[M/H] = -1.0$ (i.e. $Z=0.002$); now the derived age for the cluster is of the order of 12 Gyr. When accounting for the quoted uncertainties on both the photometric data calibration and the theoretical colour - effective temperatures relation, this result can not be considered as a plain evidence that NGC6752 has a so large metallicity (see, for instance, Vandenberg 2000). However, it is clear that a more reliable investigation on the GCs properties requires also a more accurate evaluation of the GC metallicity scale (Rutledge, Hesser & Stetson 1997), and also an homogeneous measurement of both the iron content and α -elements abundance.

4 CONCLUSIONS

In this paper we have presented new models for metal poor VLM MS stars based on the most updated physical scenario. In particular, present computations rely on the set of model atmospheres for M dwarfs recently provided by Allard et al. (1997) and Hauschildt et al. (1999). The role played by model atmospheres in predicting the observational properties of VLM stellar models has been discussed by comparing models computed under different boundary conditions. As a result, it appears that predictions about the star luminosities and radii are fairly solid whereas the predicted colours of the stellar models are critically dependent on the adopted model atmospheres which could be still affected by not negligible uncertainties (see below).

As already known, we found that the slope of the VLM sequence is sensitively dependent on the stellar metallicity. In addition, we show that the CMD location of VLM stars observed by HST in selected galactic globulars is well reproduced by theoretical stellar models. This occurrence appears as a plain evidence that present theoretical framework for VLM structures is able to finely reproduce the dependence of the observational properties of M dwarfs on the heavy elements abundance.

In this context it is worth noticing that, if and when the cluster reddening is known, the magnitude of the MS at $(V-I)_0 = 0.95$ mag, could be used as a standard candle to derive information on the cluster distance modulus and, in turn, on the cluster age. In this respect, we note

Figure 8. *Top Panel:* as figure 6 but for the cluster NGC6752. *Bottom Panel:* as top panel but by adopting for the theoretical framework a metallicity equal to $[M/H] = -1.0$ (i.e. $Z=0.002$) (see text for more details).

the small uncertainties on the cluster reddening do not play a dramatic role. In fact, present evolutionary models predict for the main sequence slope around $M_V \approx 7$ mag, $\partial M_V / \partial (V-I) \sim 4.3$. Therefore, an uncertainty in the reddening of the order of $\Delta E(V-I) \sim 0.02$ mag would imply a corresponding uncertainty in the cluster distance modulus of about $\Delta(m-M)_V \sim 0.09$ mag. According to current calibrations of the Turn Off magnitude as a function of the age (see, e.g., Cassisi et al. 1998, 1999), the quoted uncertainty would to constraint the cluster age within $\sim \pm 1.2$ Gyr.

At larger metallicities, theoretical models predict a CMD location of the MS which, for each given colour, appear slightly fainter when compared with the observations. As it has been discussed in the previous section, this occurrence can be due to a significant uncertainty in the adopted metallicity, but it can be also a first signature of a real shortcoming of the models, as shown by Baraffe et al. (1998), and confirmed by our own computations, by comparing theory and observations at solar metallicity. Following the early suggestion provided by Alvarez & Plez (1998), Baraffe et al. (1998) have shown by performing some numerical experiments, that such discrepancy between models and observations could be solved by accounting for a missing source of opacity for wavelengths shorter than $1\mu m$. It is worth noticing that an increase in the stellar opacity in this spectral range would improve the match between theory and

observations in the optical, but without affecting the near-infrared colours. This occurrence allow us to be confident in the results so far obtained in comparing VLM models with near-infrared photometric data at solar metallicity (see for instance, Zoccali et al. 1999).

ACKNOWLEDGMENTS

We gratefully acknowledge F. Allard and P.H. Hauschildt for kindly providing us with their updated "Next Generation" model atmospheres as well as for useful informations and suggestions about these models. We are also grateful to an anonymous referee for the pertinence of her/his comments regarding the content of an early draft of this paper, which significantly improved its readability.

REFERENCES

- Alexander D. R., Brocato E., Cassisi S., Castellani V., Degl'Innocenti S. & Ciacio F. 1997, *A&A*, 317, 90
- Alexander D. R. & Ferguson J. W. 1994, *ApJ*, 437, 879
- Allard F. & Hauschildt P. H. 1995, *ApJ* 445, 433
- Allard F., Hauschildt P. H., Alexander D. R. & Starrfield S. 1997, *ARAA*, 35, 137
- Alvarez R. & Plez B. 1998, *A&A*, 330, 1109
- Baraffe I., Chabrier G., Allard F. & Hauschildt P. H. 1997, *A&A*, 327, 1054
- Baraffe I., Chabrier G., Allard F. & Hauschildt P. H. 1998, *A&A*, 337, 403
- Bessel M. S. 1995, in *Proceedings of the ESO workshop "The bottom of the Main Sequence and Beyond"*, Tinney C.G., ed., p.123
- Brett J.M. 1995a, *A&A* 295, 736
- Brett J.M. 1995b, *A&ASS* 109, 263
- Brocato E., Cassisi S. & Castellani V. 1997, in "Advances in Stellar Evolution", ed. Rood R. T. & Renzini A. (Cambridge Press), p.38
- Brocato E., Cassisi S. & Castellani V. 1998, *MNRAS*, 295,74.
- Cassisi S., Castellani V., Degl'Innocenti S. & Weiss A. 1998, *A&AS*, 129 267
- Cassisi S., Castellani V., Degl'Innocenti S., Salaris M. & Weiss A. 1999, *A&AS*, 134, 103
- Castellani V., Ciacio F., Degl'Innocenti S. & Fiorentini G. 1997, *A&A*, 322, 801
- Chabrier G. & Baraffe I. 1997, *A&A*, 327, 1039
- Cohen, J. G., Gratton, R. G., Behr, B. B., Carretta, E. 1999, *in preparation*
- Cool A. M., Piotto G. P. & King, I. R. 1996, *ApJ*, 468, 655
- Drukier G.A., Fahlman G.G., Richer H.B., Searle L. & Thompson I. 1993, *AJ*, 10, 2335
- Ferraro F. R., Carretta E., Bragaglia A., Renzini A. & Ortolani S. 1997, *MNRAS*, 286, 1012
- Gratton R. G., Fusi Pecci F., Carretta E., Clementini G., Corsi C. E. & Lattanzi M. 1997, *ApJ*, 491, 749
- Hauschildt P.H., Allard F. & Baron E. 1999, *ApJ*, 512, 377
- Harris W. E. 1996, *AJ*, 112, 1487
- He L.D., Whittet D.C.B., Kilkenny D. & Jones J.H.S. 1995, *ApJS*, 101, 335
- Henry T. J & McCarthy D. W. Jr. 1993, *AJ*, 106, 773
- Holtzman J. A., Burrows C. J., Casertano S., Hester J. J., Watson A. M. & Worthey G. S. 1995, *PASP*, 107, 1065
- King I. R., Anderson J., Cool A. M. & Piotto G. 1998, *ApJ*, 492, L37
- Kroupa P. & Tout C. A. 1997, *MNRAS*, 287, 402
- Kurucz R. L. 1993, *SAO CD-ROM*
- Marconi G., Buonanno R., Carretta E., Ferraro F., Montegriffo P., Fusi Pecci F., De Marchi G., Paresce F. & Laget M. 1998, *MNRAS*, 293, 479
- Mihalas D. 1978, *Stellar Atmosphere*, 2d Ed. Freeman and Cie
- Morel P., van't Veer C., Provost J., Berthomieu G., Castelli F., Cayrel R., Goupil M. J. & Lebreton Y. 1994, *A&A*, 286, 91
- Piotto G., Cool A. M. & King I. R. 1997, *AJ*, 113, 134
- Piotto G. & Zoccali M. 1999, *A&A*, 345, 485
- Reid I. N. & Gizis J. E. 1998, *AJ*, 116, 2929
- Renzini A., Bragaglia A., Ferraro F. R., Gilmozzi R., Ortolani S., Holberg J. B., Liebert J., Wesemael F. & Bohlin R. C. 1996, *ApJ*, 465, L23
- Rogers F. J. & Iglesias C. A. 1992, *ApJS*, 79, 507
- Rogers F. J., Swenson F. J. & Iglesias C. A. 1996, *ApJ*, 456, 902
- Rutledge G. A., Hesser J. E. & Stetson P. B. 1997, *PASP*, 109, 907
- Salaris M. & Weiss A. 1997, *A&A*, 327, 107
- Salaris M., Chieffi S. & Straniero O. 1993, *ApJ*, 414, 580
- Saumon D., Chabrier G. & Van Horn H. M. 1995, *ApJS* 99, 713
- Vandenbergh D.A 2000, *ApJ*, *submitted to*
- Zoccali M., Cassisi S., Frogel J.A., Gould A., Ortolani S., Renzini A., Rich R.M. & Stephens A.W. 2000, *ApJ*, *in press*

This paper has been produced using the Royal Astronomical Society/Blackwell Science \TeX macros.

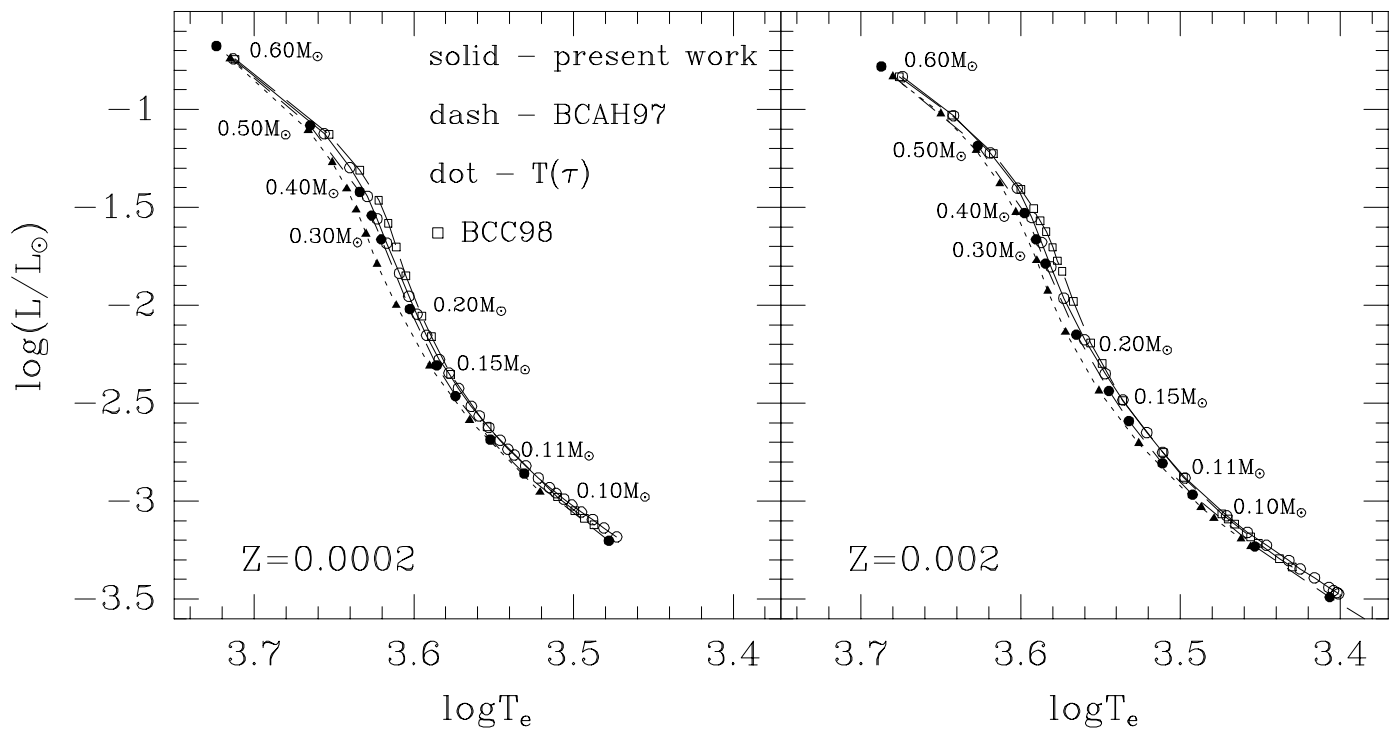


Figure 1

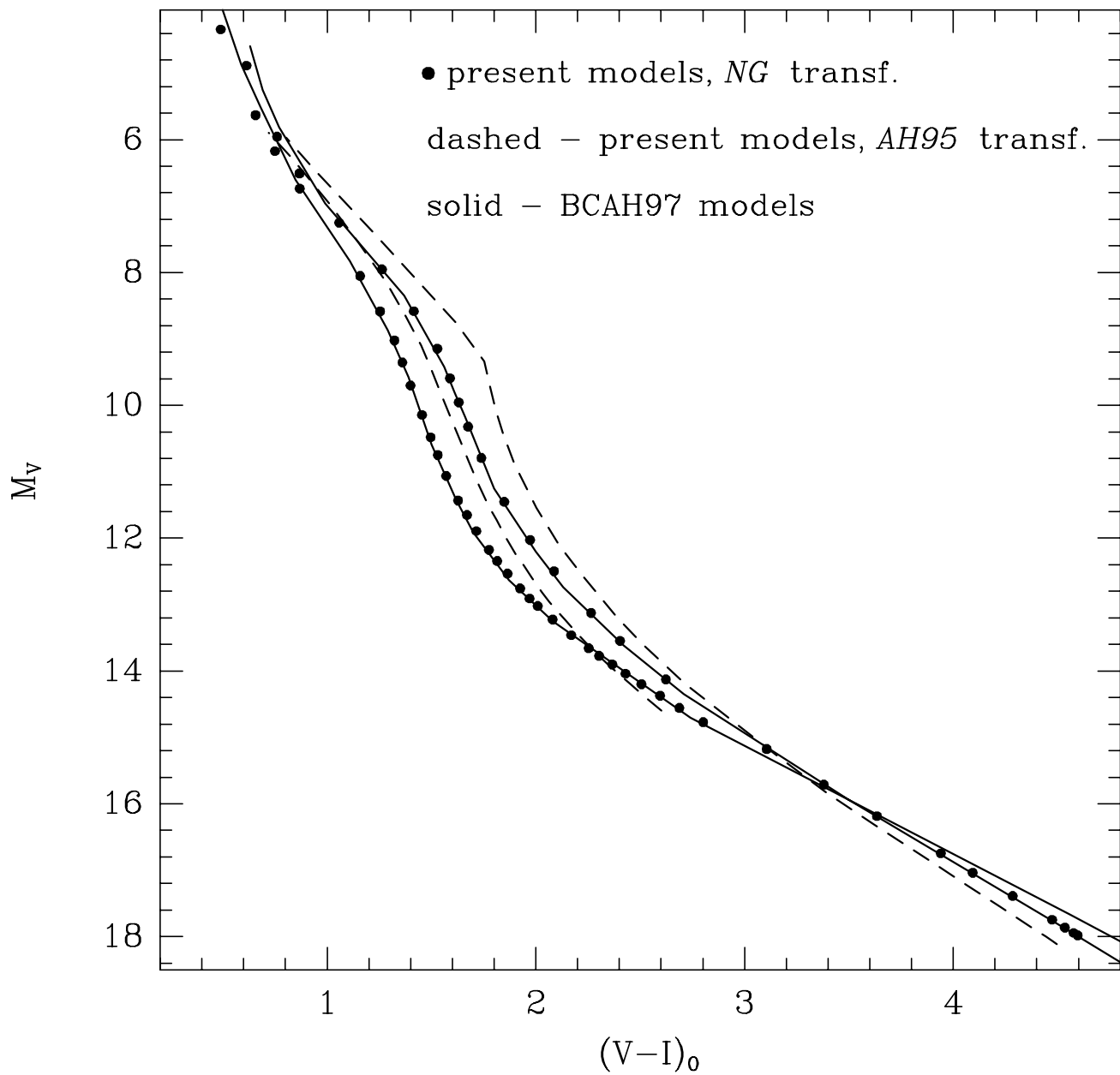


Figure 2

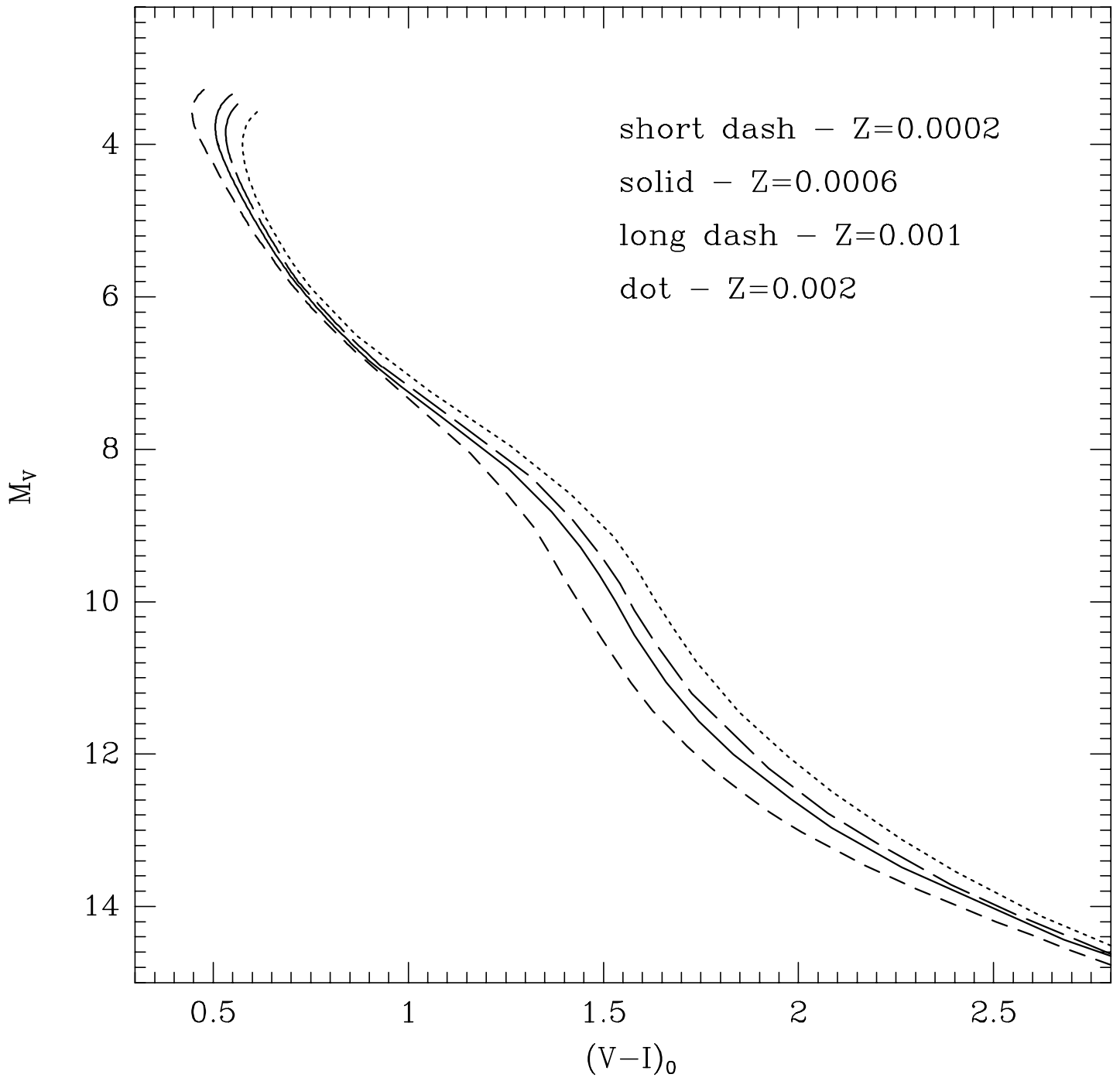


Figure 3

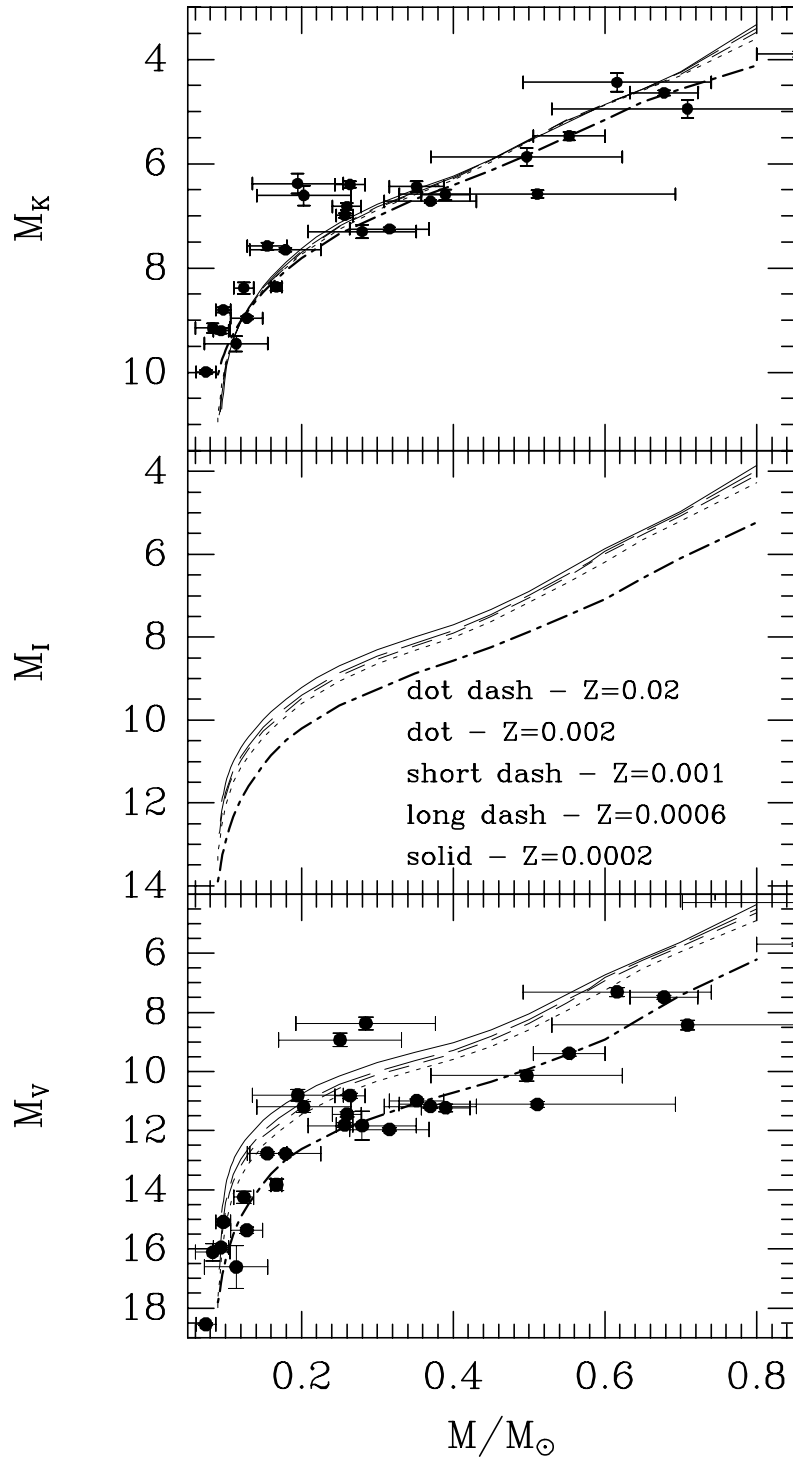


Figure 4

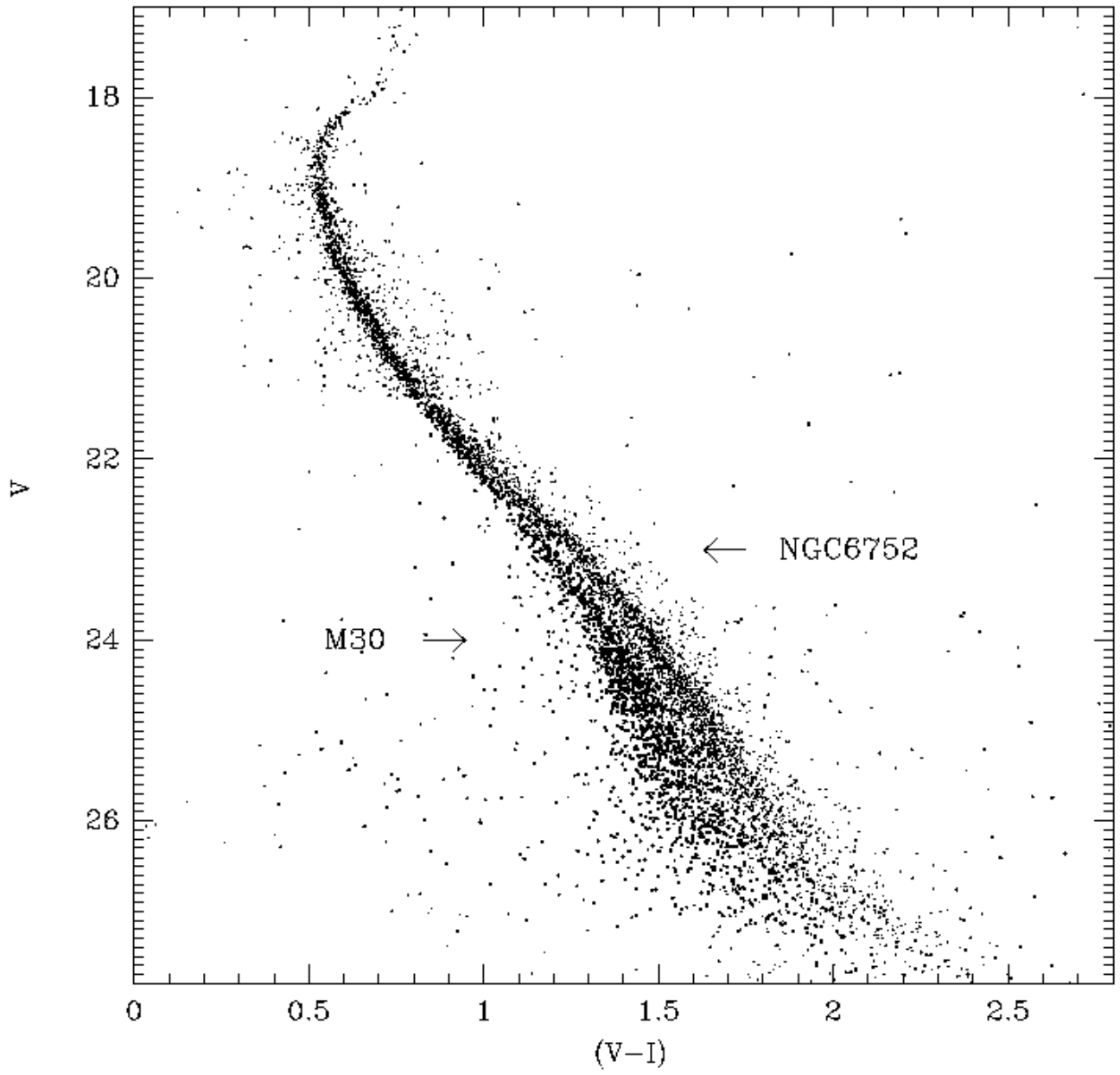


Figure 5

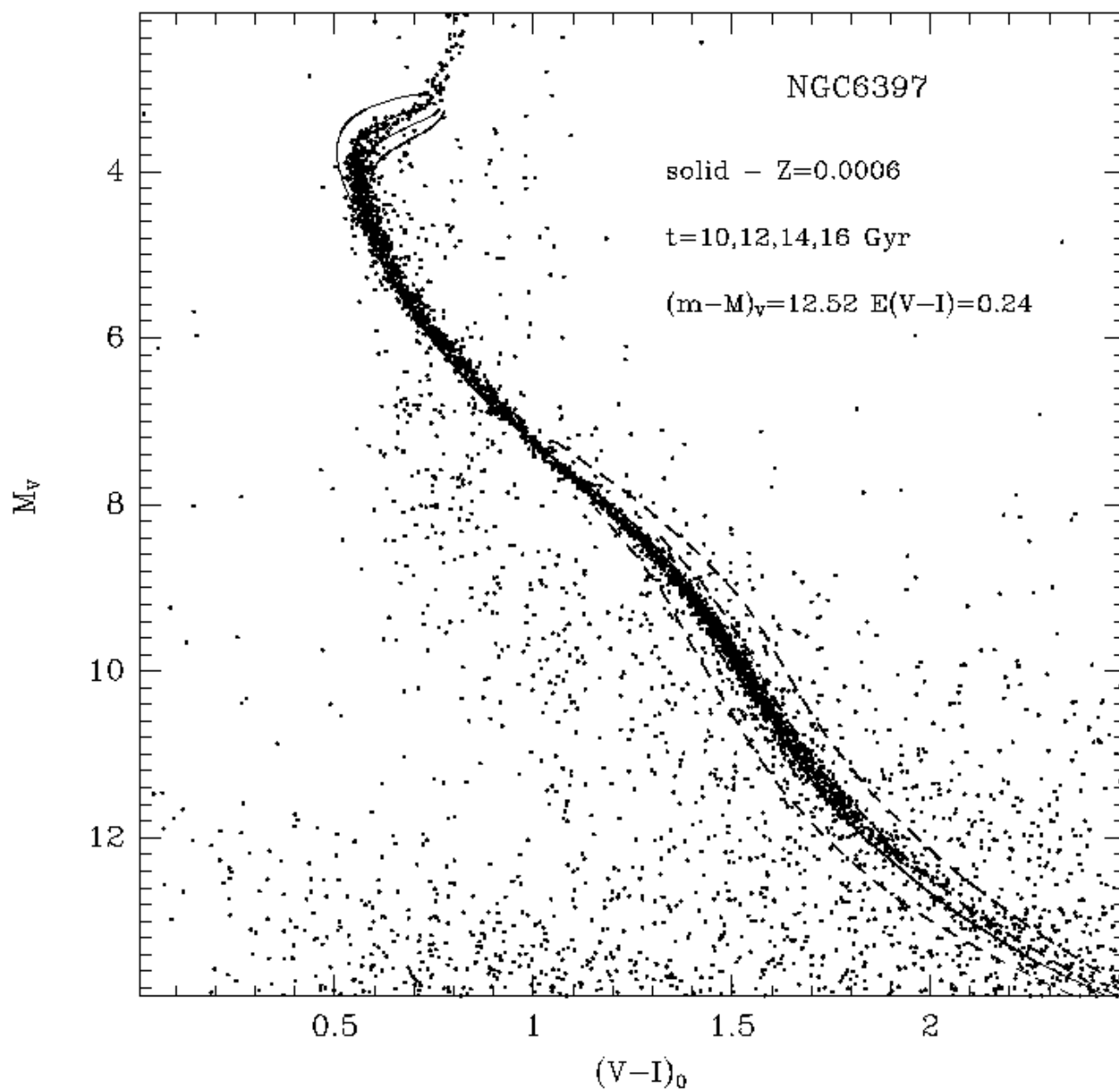


Figure 6

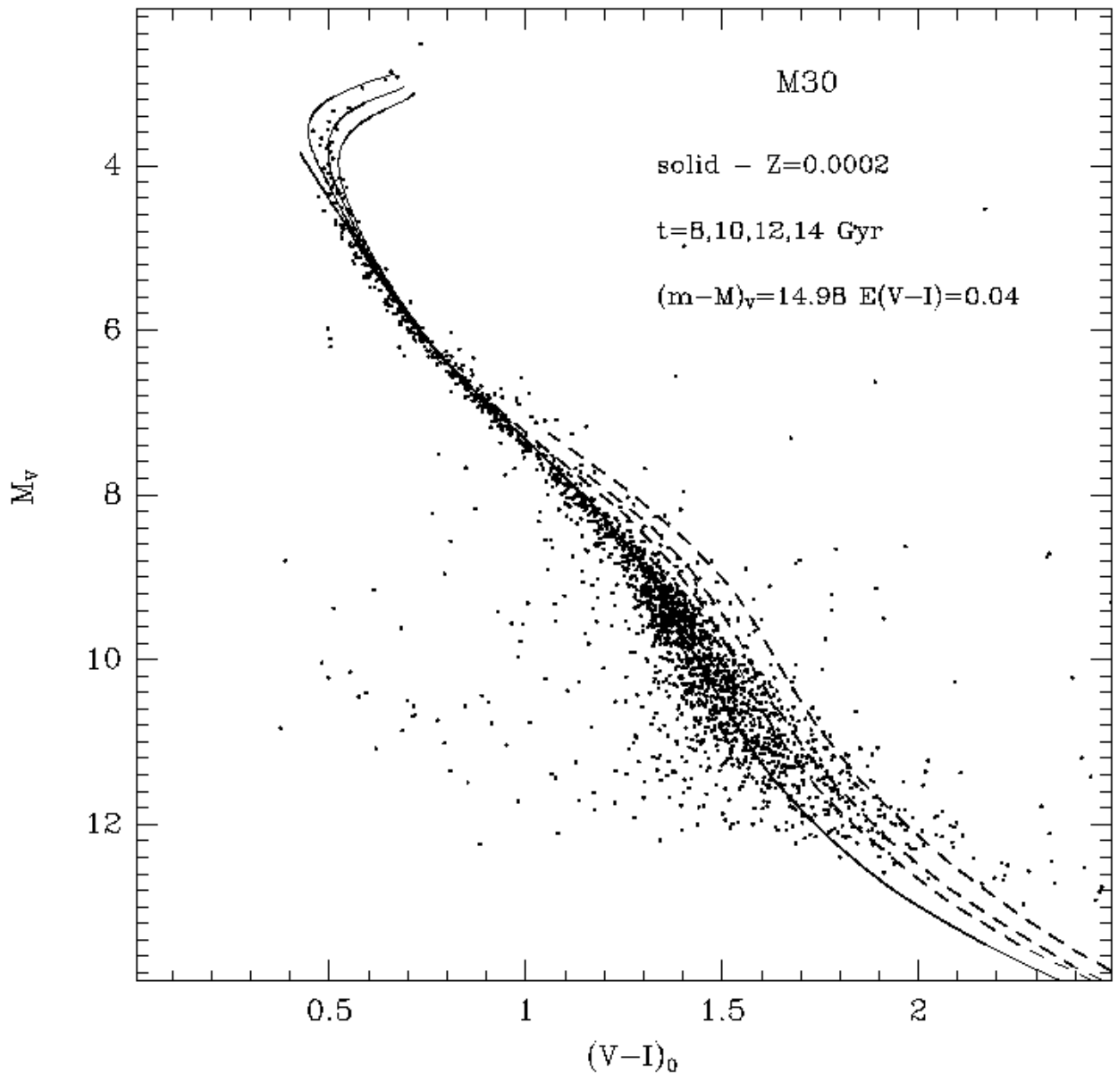


Figure 7

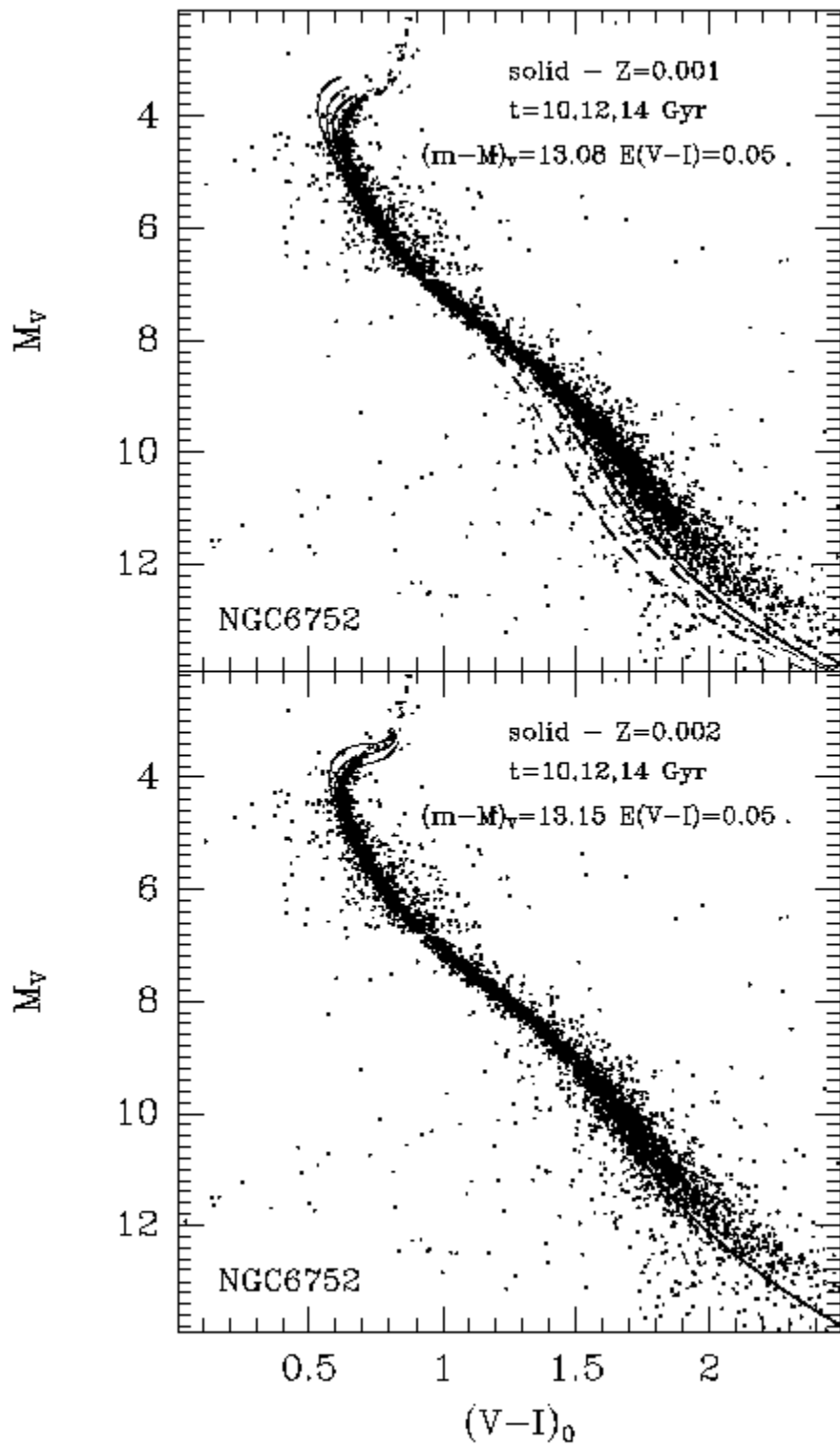


Figure 8